Original Article

The International Journal of Lower Extremity Wounds
1–10

DOI: 10.1177/1534734620921629
journals.sagepub.com/home/ijl
SAGE

Development and Characterization of Squalene-Loaded Topical Agar-Based Emulgel Scaffold: Wound Healing Potential in Full-Thickness Burn Model

T. S. Shanmugarajan, MPharm, PhD[1], N. Kalai Selvan, MPharm[1], and Varuna Naga Venkata Arjun Uppuluri, MPharm[1]

Abstract

Full-thickness burns pose a major challenge for clinicians to handle because of their restricted self-healing ability. Even though several approaches have been implemented for repairing these burnt skin tissue defects, all of them had unsatisfactory outcomes. Moreover, during recent years, skin tissue engineering techniques have emerged as a promising approach to improve skin tissue regeneration and overcome the shortcomings of the traditional approaches. Although previous literatures report the wound healing effects of the squalene oil, in the current study, for the first time, we developed a squalene-loaded emulgel-based scaffold as a novel approach for potential skin regeneration. This squalene-loaded agar-based emulgel scaffold was fabricated by using physical cross-linking technique using lecithin as an emulsifier. Characterization studies such as X-ray diffraction, Fourier-transform infrared spectroscopy, and field emission scanning electron microscopy revealed the amorphous nature, chemical interactions, and cross-linked capabilities of the developed emulgel scaffold. The squalene-loaded emulgel scaffold showed excellent wound contraction when compared with the agar gel and negative control. In case of the histopathology and recent immunohistochemistry findings, it was clearly evidenced that squalene-loaded emulgel promoted faster rate of the revascularization and macrophage polarization in order to enhance the burn wound healing. Moreover, the findings also revealed that the incorporation of squalene oil into the formulation enhances collagen deposition and accelerates the burnt skin tissue regeneration process. Finally, we conclude that the squalene-loaded emulgel scaffold could be an effective formulation used in the treatment of the burnt skin tissue defects.

Keywords

emulgel scaffold, squalene, agar, wound healing, tissue regeneration

Introduction

Skin tissue is a well-organized structure within our body that possesses excellent biomechanical properties such as friction and tensile strength. However, burnt skin tissue is challenging to repair because of its lack of blood vessels or lymphatic vessels. Hence, self-healing is the major and challenging obstacle for tissue regeneration in case of burnt skin tissue.[1,2] Ideally, burnt skin tissue defects can be repaired with biomaterials showing excellent biomimetic properties and extracellular matrix support.[3-6] Moreover, the limitations of current treatment modalities, such as autograft and allograft, in the regeneration of the functional skin tissue paved the way for tissue engineering concepts in the burnt wound management.[7-10]

Now a days, scaffolds play a significant role in tissue regenerative concepts. Moreover, these scaffolds are known to be natural/semisynthetic/synthetic supportive materials that usually act as a vehicle for several drug molecules and growth factors. Since the past few decades, the functional modification of a scaffold is a major focus area in burnt skin tissue regeneration.[11,12] Whereas currently in the formulation of an emulgel scaffold focus is on natural materials because of their excellent biocompatibility and biodegradability. Basically, emulgels are cross-linked networks formed by combining the emulsion and gel-based system.[13]

[1]Vels Institute of Science, Technology & Advanced Studies, Chennai, India

Corresponding Author:
T. S. Shanmugarajan, Department of Pharmaceutics, School of Pharmaceutical Sciences, Vels Institute of Science, Technology & Advanced Studies, Pallavaram, Chennai 600117, India.
Email: shanmuga5@yahoo.com

However, excellent biomaterials and adequate fabrication methods are essential for the development of an ideal emulgel scaffold. Furthermore, the present study on emulgel scaffold is one of its kind that plays a vital role in skin tissue regeneration.

In the current study, natural polymer like agar was used as a gelling agent because of its role in development of the enthalpically stabilized inter-chain linkages. However, in our previous study, it was demonstrated that these linkages were essential for promotion of 3-dimensional scaffolding structures.[14] Moreover, the excellent biocompatibility and biodegradability of the agar molecule showed its importance in the regenerative medicine–related formulations.[15-17] Coming to the emulsifiers, these represent the indispensable part of an emulgel formulation; basically the choice of emulsifier can strongly affect emulgel performance. However, in the current study, lecithin enhances the stability by preventing the creaming effect within the formulation. Hence, due to this reason it found its importance in the emulgel formulation.[18-22]

Squalene, a terpenoid derivative, was an intermediate compound obtained during the synthesis of cholesterol and commercially isolated from soya that exhibits the structural similarity toward carotenoid. It seems to protect the skin tissue from oxidative stress.[23] The objective of the present study was to demonstrate the fabrication of the squalene oil–loaded emulgel scaffold via rapid physical cross-linking technique and assess its potential in burn wound healing. Furthermore, the agar gel and squalene-loaded emulgel scaffold were characterized by X-ray diffraction (XRD), Fourier-transform infrared (FTIR) spectroscopy, field emission scanning electron microscopy (FESEM), in vivo studies, in vitro studies, histopathological analysis, Masson's trichome staining, CD68 staining, and Ki67 staining.

Materials and Methods

Materials

Squalene 98% (GC) and lecithin from soya were obtained from Tokyo Chemical India Pvt. Ltd (Chennai, India). Agar-Agar powder was obtained from HI-media. All the samples we used in this study were obtained from genuine sources and were used as such.

Preparation of Squalene-Loaded Emulgel Scaffold

In the current study, the squalene-loaded emulgel scaffold was fabricated by using physical cross-linking technique. Initially, squalene oil (4% W/W [weight/weight]) was emulsified by using the lecithin as an emulsifying agent. Later, 2 g of agar was dissolved in distilled water under continuous reflux. Finally, emulsified squalene was loaded into the previously homogenized 0.5% agar solution at 80°C with continuous stirring. After continuous stirring for about 2 hours, the formulation was placed at 37°C for about 24 hours. Moreover, in this study, thermostat played a significant role in maintaining the stable temperature.

X-Ray Diffraction Study

The crystalline/amorphous nature of the prepared emulgel scaffold was determined using the XRD study. XRD patterns of freeze-dried agar gels and squalene-loaded emulgels were analyzed using Bruker D8 Advance X-ray diffractometer having the scanning range width (2θ) of about 10 to 80 with a step-width of about 0.003.[24-28]

FTIR Analysis

FTIR spectra of squalene-loaded emulgel scaffold and agar gel were characterized by using KBr disk method. FTIR spectroscopy was conducted using a Perkin Elmer Spectrum 100 spectrometer equipped with ATR (attenuated total reflectance) with a resolution of 4 cm^{-1}, in the range of 4000 to 400 cm^{-1}, with 32 scans to further characterize the fine components of the samples. Prior to FTIR characterization, samples were freeze-dried for 72 hours and about 1 mg of squalene-loaded emulgel scaffold and agar gels was used for this study.[26,28-33]

Field Emission Scanning Electron Microscopy

Both the agar gel and squalene-loaded emulgel were lyophilized and platinum-coated surfaces before a SEM (S-4700, Hitachi Limited, Japan) at 20 kV was used to observe their morphology.[32-35]

In Vivo Studies

Twenty-four healthy male Wister albino rats were divided into 3 groups, each group comprising 8 rats, for evaluating the burn wound healing potential. The animal study was approved by the Institutional Animal Ethical Committee of Vels University, Chennai, India.

In order to test the wound healing potential of the squalene oil–loaded emulgel scaffold, burnt tissue defects of 10 mm in diameter were developed on the dorsal surface of the male Wister albino rats, in which Group A represents negative control, Group B represents agar gel, and Group C represents squalene oil–loaded emulgel scaffold. Later, all the groups were monitored at predetermined time points for wound closure.[36-39]

Histopathological Analysis

For histopathological research, the granulation tissues obtained on days 4, 8, and 12 were used. Samples of tissue were fixed in 10% formalin, dehydrated in graded alcohol series, washed in xylene, and coated in paraffin wax. Then,

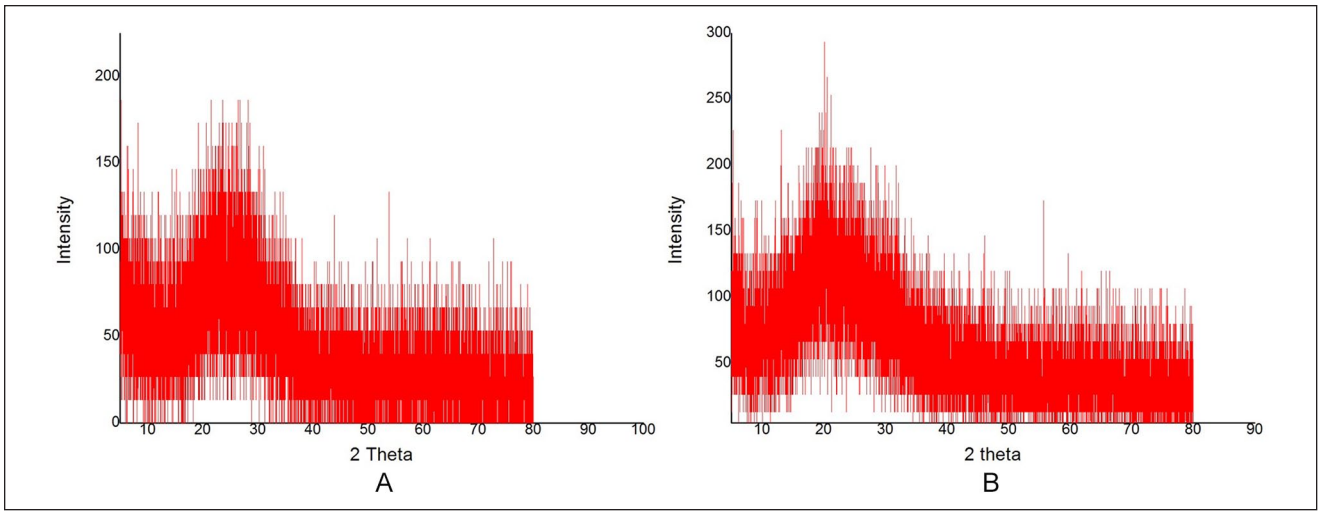

Figure 1. The X-ray diffraction (XRD) pattern of various polymers and drug molecules. (A) XRD of agar gel and (B) XRD of squalene-loaded emulgel scaffold.

the samples were cut and mount in serial sections (4-µm thickness) on glass slides. Later, hematoxylin-eosin and Masson's trichrome stain stained the tissue sections. Finally, the stained tissue sections were examined for histological study under a light microscope (Olympus-IX 51).[40-43]

Ki67 and CD68 Immunohistochemistry

Tissue sections were trimmed at 4 µm, deparaffinized with xylene and ethanol, and further incubated for 10 minutes in 3% H_2O_2. After washing in distilled water, a vegetable steamer was used to incubate the slides at 95°C for 25 minutes in citrate buffer pH 6 (Invitrogen, Carlsbad, CA). The slides were rinsed in PBS-containing 0.05% Tween-20 (PBST) and then incubated overnight at room temperature with 1:100 Ki67, CD68 antibody (DAKO, Carpinteria, CA) at 4°C. Then, all the Ki67- and CD68-stained slides were rinsed with PBST and incubated with 1:200 polyclonal rabbit anti-rat immunoglobulin/biotinylated Ab (Dako) at room temperature for 30 minutes. Later, all slides were rinsed with PBST and incubated at room temperature for 30 minutes with Dako EnVision+ System—HRP Labelled Polymer Anti-Rabbit (Dako). Furthermore, in the current study, all the slides were incubated for visualization with DAB (3,3′-diaminobenzidine). Eventually, after rinsing under tap water, all the slides, 4th, 8th, 12th day tissue sections, were counter-stained with Harris' hematoxylin, dehydrated in ethanol, and finally were mounted with media.[27,44-51]

Results

X-Ray Diffraction

In the current study, XRD patterns of agar gel and squalene-loaded emulgel scaffold were studied in the scanning range of $5° \leq 2\theta \leq 90°$. In case of agar gel (Figure 1A), the amorphous nature of the XRD peak was clearly observed. Moreover, in case of agar gels, the XRD patterns showed peak (2θ) at 24° with an intensity of 186. Whereas in case of the squalene-loaded emulgel scaffold (Figure 1B), XRD patterns show peak at 20° with an intensity of 293. Moreover, in the present study, even though there was no change in the amorphous state of both agar gel and squalene-loaded emulgel scaffold, a slight shift in the intensity peak was identified in case of the XRD patterns of the squalene-loaded emulgel scaffold.

Fourier-Transformed Infrared Spectroscopy

The FTIR spectra of the agar gel and squalene-loaded emulgel scaffold are presented in Figure 2. In case of agar gel (Figure 2A), the broad range of the absorption at 3363 cm^{-1} was mainly due to the presence of the hydrogen bonding at OH group stretch. The peak at 2917 cm^{-1} was considered to be C–H stretching. The appearance of peak at 1645 cm^{-1} was referred as C=C bond. However, the peak at 1645 cm^{-1} was also considered to be the characteristic peak for polysaccharides and this further substantiates the presence of agar.

Whereas in case of the squalene-loaded emulgel scaffold (Figure 2B) the absorption band at 3378 cm^{-1} was mainly due to the presence of the OH group, and the absorption peak at 2920 cm^{-1} mainly corresponds to asymmetric stretching of C–H group. Moreover, the absorption band at 1642 cm^{-1} represents the characteristic polysaccharide peak and this was associated with the existence of the agar within the squalene-loaded emulgel scaffold. Furthermore, the additional peaks at 1254 cm^{-1} and 1150 cm^{-1} represent C–N and C–O stretching, respectively.

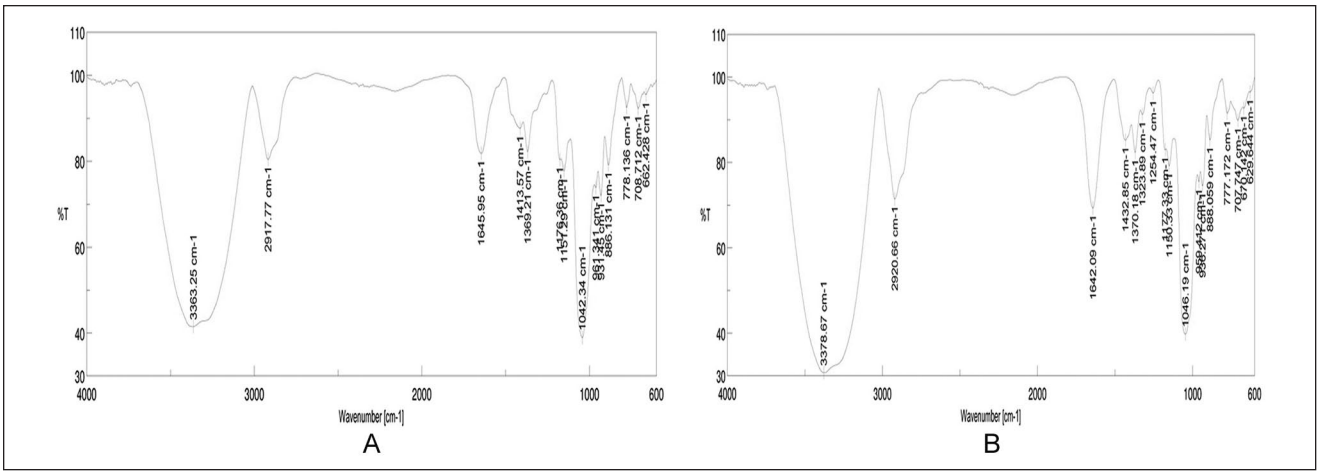

Figure 2. Fourier-transform infrared (FTIR) spectrum of polymers, drug, and hydrogel scaffolds. (A) FTIR of agar gel and (B) FTIR of squalene-loaded emulgel scaffold.

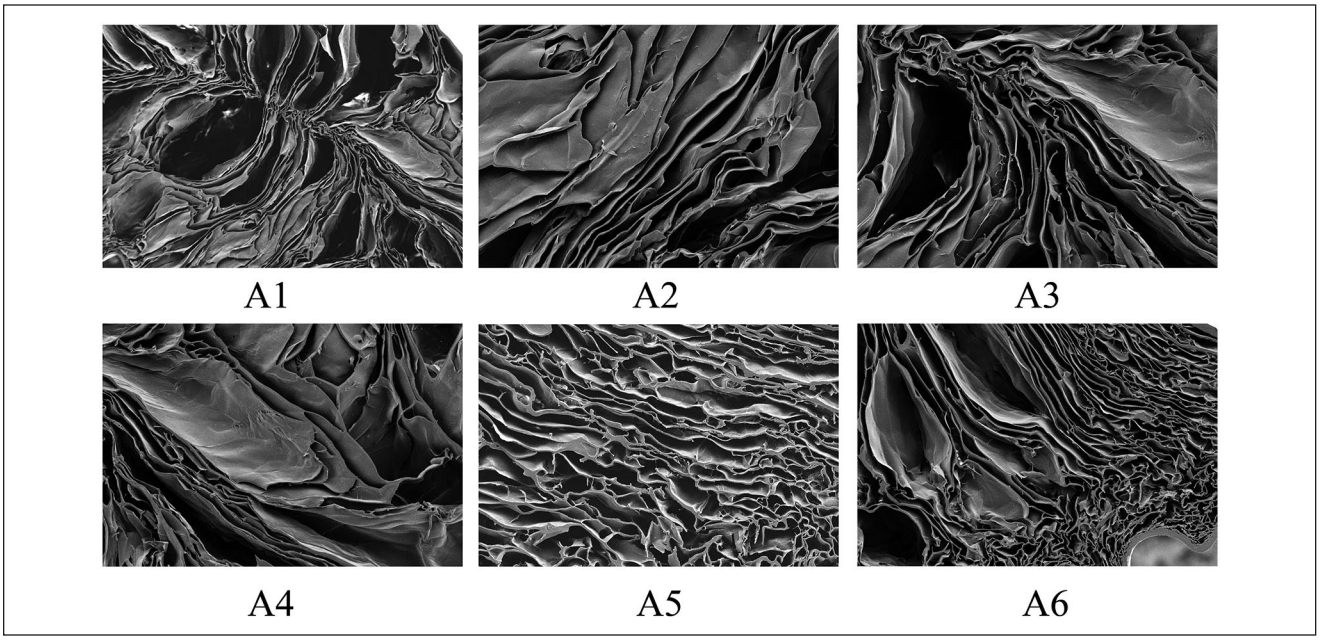

Figure 3. Field emission scanning electron microscopy (FESEM) images of agar gels. A1 represents FESEM image focused at 200 µm and magnification was about 150×. A2 represents image at 30 µm with magnification 500×. A3 represents image at 100 µm with magnification 453×. A4 represents the image at 100 µm with magnification 396×. A5 represents the image at 20 µm with magnification 1000×. A6 represents the image at 20 µm with magnification 500×.

Field Emission Scanning Electron Microscopy

FESEM studies usually describe the extent of cross-linkage that exists within the developed emulgel scaffold. In the current study, in case of the agar gels (Figure 3), it demonstrated that cross-linked network–like structure made this molecule useful for the development of emulgel scaffold. Moreover, in case of squalene-loaded emulgel scaffold (Figure 4), it was clearly evidenced that the squalene oil shows excellent spreadability within the porous gaps of freeze-dried agar gels. Thus, after visualizing the FESEM image of squalene-loaded emulgel scaffold, it can be said that there exists an excellent interaction between squalene and agar.

In Vivo Studies

Burnt skin tissues at predetermined time points were harvested for gross evaluation of in vivo burnt tissue repair. Figure 5 depicts the possible skin tissue regeneration approaches of our formulation. In Figure 5, 4A to 4C refer to the negative control, agar gels, and squalene-loaded

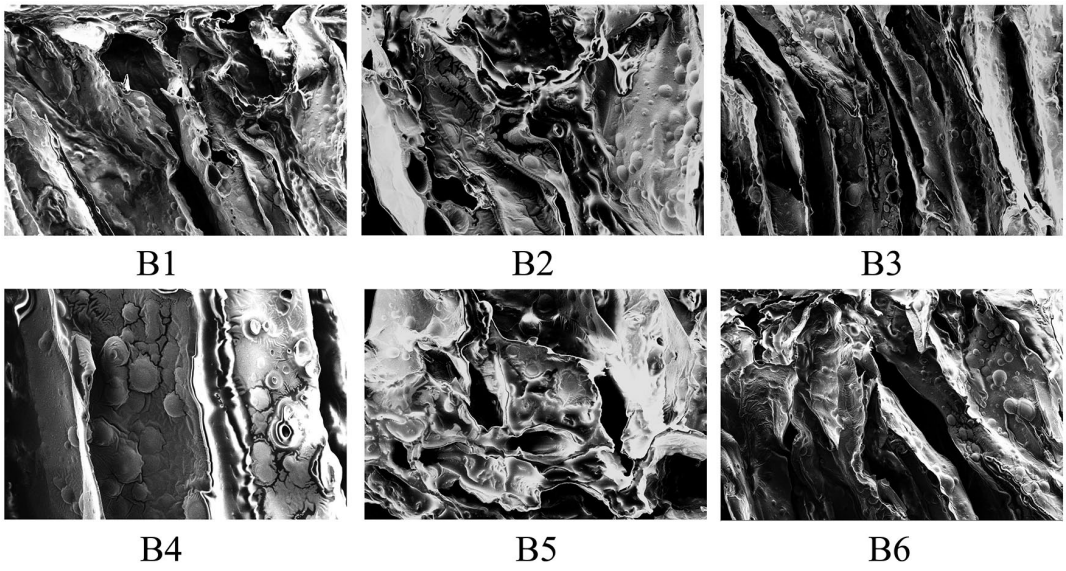

Figure 4. Field emission scanning electron microscopy (FESEM) image of squalene-loaded emulgel scaffold. B1 represents FESEM image focused at 100 µm with magnification of 251×. B2 represents the image at 20 µm with magnification of 500×. B3 represents image at 200 µm with magnification of 200×. B4 represents image at 20 µm with magnification of 800×. B5 represents image at 20 µm with magnification of 501×. B6 represents image at 100 µm with magnification of 316×.

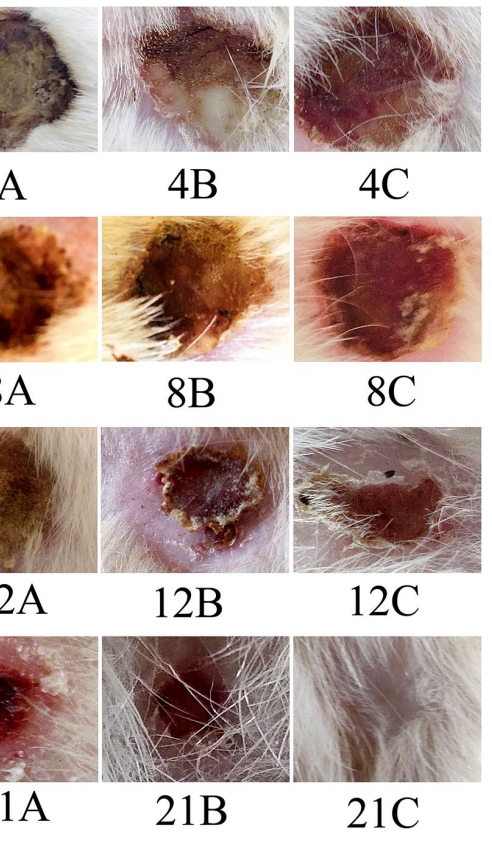

Figure 5. In vivo release studies. Number of days represented by 4, 8, and 12 days. (A) Negative control, (B) agar gel, and (C) squalene-loaded emulgel scaffold.

emulgel scaffold at the fourth day. At the fourth day, in case of negative control, no significant improvement was seen. But, however, on comparison with the agar gels, the squalene-loaded emulgel scaffold exhibited excellent granulating tissue. In Figure 5, 8A to 8C depict the negative control, agar gels, and squalene-loaded emulgel scaffold at the eighth day. When compared with the fourth day groups, all the eighth day samples displayed significant development in terms of new tissue formation. However, significant reepithelization was seen in case of squalene-loaded emulgel scaffold when compared with the negative control and agar gel. In Figure 5, 12A to 12C depict that in the 12th day samples the inflammation was still observed in the negative control. Moreover, it was also found that there was a significant decrease in wound diameter in case of rats treated with squalene-loaded emulgel scaffold when compared with the rats treated with agar gels.

Finally, on completion of 21 days of treatment, it was clearly evidenced that in case of squalene-loaded emulgel scaffold–treated group, a scarless skin tissue had grown uniformly with the neighboring tissue. But in case of agar reepithelization, the process was not completed. Furthermore, the nonrepaired skin tissue sections still existed in the negative control. Furthermore, in the current study, Table 1 represents the wound contraction diameter (mm) of the entire treatment course.

Histopathological Analysis

Hematoxylin-eosin and Masson's trichome staining results are presented in Figure 6. Moreover, in the current study,

Table 1. The Wound Contraction Diameter (mm) of the Entire Treatment Course.

Days	Negative Control (mm)	Agar Gel (mm)	Squalene-Loaded Emulgel (mm)
0	10	10	10
4	9.4 ± 0.9	8.6 ± 0.8	7.8 ± 0.4
8	7.5 ± 0.7	6.3 ± 0.9	5.2 ± 0.6
12	6.9 ± 0.9	3.7 ± 0.3	2.6 ± 0.2
21	2.9 ± 0.3	0.2 ± 0.5	0.1 ± 0.3

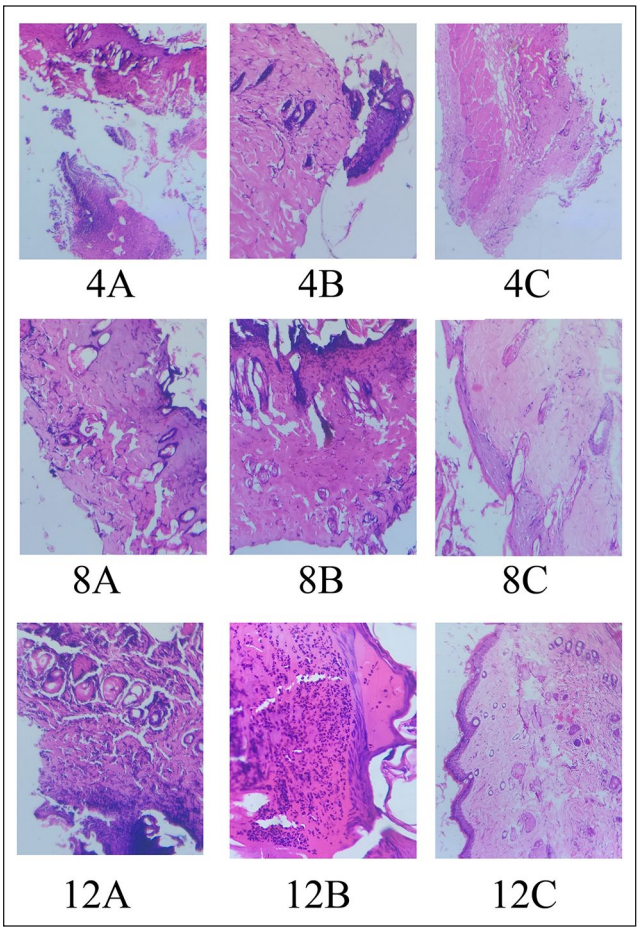

Figure 6. The 100× magnification image of hematoxylin-eosin staining represented by 4, 8, and 12 days. (A) Negative control, (B) agar gel, and (C) squalene-loaded emulgel scaffold.

when compared with the negative control- and agar gel–treated tissue sections, squalene-loaded emulgel scaffold–treated tissue sections had shown significant rate of tissue regeneration. In case of negative control tissue sections during the fourth and eighth days, prolonged rate of inflammation was seen. Finally, during the 12th day, minimal amount of collagen content was evidenced in the tissue sections of the negative control.

Fourth day agar gels–treated tissue sections revealed about the fibroblast formation with minimal amount of collagen. Later, on the eighth day, agar gels–treated burnt wound tissue sections demonstrated a narrow epithelial layer and lesser capillary formation. Furthermore, on the 12th day, when compared with the negative tissue sections, the agar gel tissue sections showed enormous blood capillaries and fibroblasts, indicating a better angiogenic response.

In the current study, squalene-loaded emulgel scaffold–treated group appeared promising to granular tissue formation and also demonstrated the faster rate of reepithelization when compared with the negative control and agar gels. However, during the fourth day, significant rate of the fibroblast formation along with collagen content was evidenced in the current study. Moreover, the eighth day studies further revealed that there was a well-defined granulation tissue formation with adequate capillary formation and collagen content in case of the squalene-loaded emulgel scaffold–treated tissue sections. Finally, 12th day studies further confirmed that the squalene-loaded emulgel scaffold–treated tissue sections showed excellent reepithelization along with neovascularization and significant rate of collagen.

In the current study, in order to identify the extent of collagen formation within the isolated tissue sections, Masson's trichome staining (Figure 7) was performed. After staining all the tissue sections, it was clearly evidenced that squalene-loaded emulgel scaffold–treated sections showed significant amount of collagen when compared with agar gel–treated and negative sections.

CD68 Immunohistochemistry

Immunohistochemical staining of CD68 (Figure 8) was used to demonstrate the effect of the squalene-loaded emulgel scaffold on the macrophage polarization. Moreover, this staining was helpful in determining the extent of the inflammation within the tissue sections. At the fourth day, in case of negative control, agar gels, and squalene-loaded emulgel scaffold, early stage of inflammation was shown and this led to increase in the number of inflammatory cells like neutrophils and macrophages within the tissue sections.

Eighth day reports revealed that there was no change in inflammation in case of negative control tissue section, whereas in case of the agar gels, inflammation was reduced, but in case of the squalene-loaded emulgel scaffold, reduction in CD68 macrophages was observed.

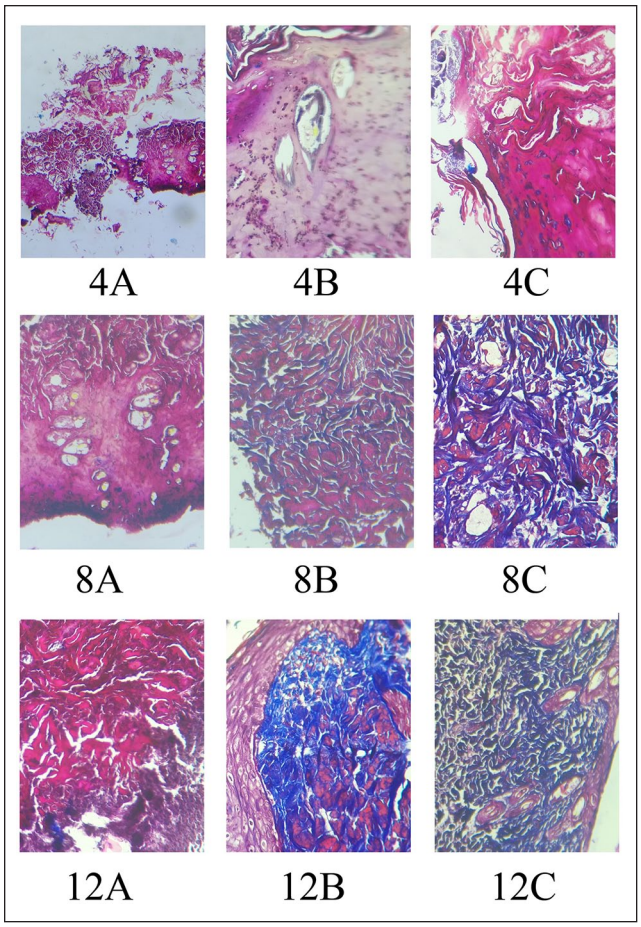

Figure 7. The 100× magnification image of Masson's trichome staining represented by 4, 8, and 12 days. (A) Negative control, (B) agar gel, and (C) squalene-loaded emulgel scaffold.

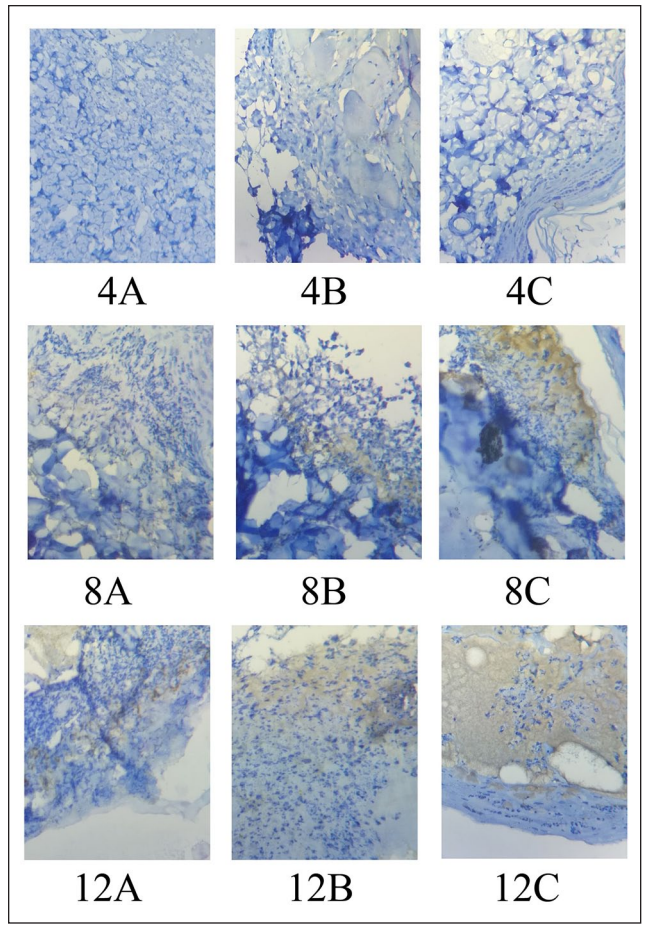

Figure 8. The 100× magnification image of CD68-stained tissues that show the infiltration of macrophages/monocytes on days 4, 8, and 12. (A) Negative control, (B) agar gels, and (C) squalene-loaded emulgel scaffold.

Finally, the 12th day findings demonstrated that squalene-loaded emulgel scaffold shows significant reduction in CD68 macrophages when compared with agar gels and negative control tissue sections.

Ki-67 Immunohistochemistry

In order to assess the role of squalene-loaded emulgel scaffold in keratinocyte proliferation, the Ki-67 immunohistochemical staining (Figure 9) was performed. Fourth day immunohistochemical staining demonstrated that a very little amount of keratinocytes proliferation was seen in case of squalene-loaded emulgel scaffold when compared with the agar gels and negative control.

Eighth day Ki-67 staining results revealed that the negative control does not show any keratinocyte proliferation. On comparison with the agar gels, the squalene-loaded emulgel scaffold had shown optimal rate of keratinocyte proliferation.

Furthermore, the 12th day Ki-67 staining revealed that significant rate of keratinocyte proliferation along with excellent wound healing was observed in case of squalene-loaded emulgel scaffold when compared with the agar gels.

Discussion

Skin is a complex structure composed of epidermis, dermis, and hypodermis, and it shows various essential structures and physiological features. Moreover, burnt tissue defects usually involve all the layers of the skin; hence, a biomimetic emulgel scaffold is needed in order to satisfy the requirements of skin tissue regeneration. Furthermore, the biomaterials selected for the burnt tissue repair should have appropriate biodegradability and ideal reepithelization.[3-6] Previously, icariin-loaded polyvinyl alcohol/agar hydrogel was produced by our group. These hydrogel scaffolds were able to promote tissue regeneration in case of rat burnt wound model.[14] On the basis of these outstanding outcomes, we chose agar as the promising polymer for enhancing the mechanical support in case of the squalene-loaded emulgel scaffold. Moreover, in the current study, glucosidyl linkage within the agar molecule

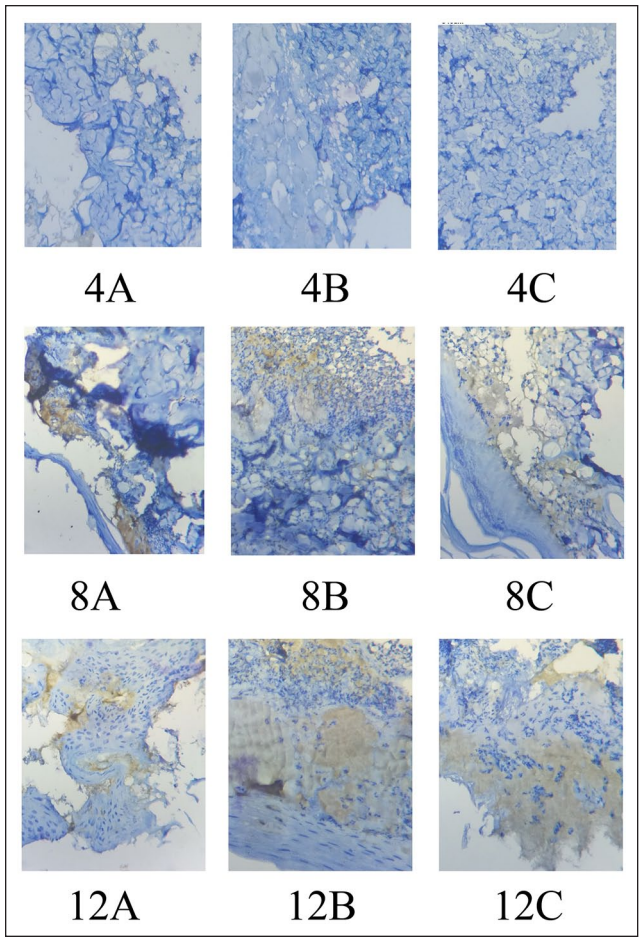

Figure 9. The 100× magnification image of immunohistochemical analysis of the presence of Ki-67 in burn wounds on days 4, 8, and 12. (A) Negative control, (B) agar gels, and (C) squalene-loaded emulgel scaffold.

plays a vital role in enhancing the gelling property and biocompatibility of the emulgel scaffold.[13,16]

To the best of our understanding, it was the first squalene oil–loaded emulgel scaffold developed with facile procedures for in vivo burnt tissue repair on dorsal region of the Wister albino rats.[38,39,52,53] Moreover, ideal mechanical properties enabled the squalene-loaded emulgel to be applied as a topical biomaterial, with the merits of minimal invasive and bio-adhesiveness as a main scaffold in skin tissue regeneration.[19-21] In the current study, FESEM studies revealed the extent of cross-linking capability of the developed agar gel; moreover, in this study, it was also justified that interconnected networks of the agar gels were essential for entrapment of the squalene oil globules.[34-37]

In the present study, XRD analysis was useful for demonstrating the physical state and compatibility of both squalene-loaded emulgel scaffold and agar gel. Moreover, the XRD patterns of these 2 samples do not show any kind of sharp peaks and this serves as an evidence for amorphous nature of the agar gel and squalene-loaded emulgel scaffold.[26-28]

Whereas the presence of squalene in emulgel scaffold formulation was verified by using FTIR spectral analysis. Furthermore, the results acquired from FTIR spectroscopy also showed that agar and squalene interacted considerably. Moreover, in the present study, in case of Figure 2B of the FTIR spectral analysis, the slight deflection in the characterization peak was due to the inclusion of the squalene into the agar.[29-31]

Histopathological findings further substantiated the tissue regeneration within the damaged burnt skin portions. Moreover, the results indicate that when compared with negative control and agar gels, this squalene-loaded emulgel scaffold was not only biodegradable but also favors the cellular proliferation with excellent extracellular matrix.[40-43]

Furthermore, in the burnt wound-healing studies, it was clearly evidenced that the prolonged inflammation, increased neutrophils, and decreased macrophages were responsible for impaired wound healing. Interestingly, in the current study, CD68 immunohistostaining plays a significant role in demonstrating the macrophage activity in wound healing process. During the wound healing, the impingement of the macrophages and neutrophils on to the wound bed was found to be the crucial for the inflammation stage. Finally, during the maturation stage, major inflammatory cells like macrophages engulfs the neutrophils by a process known as apoptosis.

Moreover, the advent of macrophages at the wound site plays a significant role in skin tissue regeneration. Previous studies about the macrophages also confirmed that because of their functional phenotypes, these macrophages play a wide range of roles in the wound healing process. Furthermore, the depletion of the macrophages during the early stages of the proliferation results in the development of severe hemorrhage, and this later during the tissue maturation stage delays the burnt wound contraction. However, in the maturation stage, the reduced macrophage count does not show a significant impact on the wound closure. In accordance with these results, during the early stage of the wound healing process, when compared with the negative control and agar gels, the squalene-loaded emulgel scaffold–treated burnt wound injuries show a high influx of macrophages, and later during the maturation stage of wound healing, macrophage count was decreased due to the anti-inflammatory activity of the squalene.[27,48-51]

In the current research, when compared with the agar gels and negative control, the squalene-loaded emulgel scaffold endorsed a solid rise in Ki-67 cells. Moreover, this Ki-67 immunohistostaining was essential for identification of granular tissue formation and neovascularization during the burn wound-healing process. In the previous literatures, it was shown that macrophage deficiency was associated with minimal angiogenesis in burnt wound injuries. Whereas our current study reports that Ki-67 cells were increased at the squalene-loaded emulgel scaffold–treated burnt wound sites when compared with the burnt wound sites treated with

agar gels and negative control. This further indicated that squalene-loaded emulgel scaffold–treated burnt wound site shows excellent cellular proliferation by improving the recruitment of the macrophages during the proliferation and maturation stages of burnt wound-healing process. Finally, these findings demonstrated the beneficial effects of squalene-loaded emulgel on enhanced angiogenic response and cellular proliferation. Thus, it was confirmed that squalene-loaded emulgel scaffold can be helpful for curing full-thickness burn injuries.[44,46]

Overall, squalene-loaded emulgel scaffold treatment resulted in excellent reepithelization, neovascularization, and angiogenic response when compared with the agar gels and negative control treatments in the burnt wound rats.

Conclusion

In this study, we revealed the feasibility of preparing the squalene-loaded emulgel scaffold for burnt skin tissue regeneration using an innovative rapid physical cross-linking method. When topically applied on to the damaged skin portions, the squalene-loaded emulgel scaffold showed excellent matrix support and allowed the reepithelization of the burnt skin portions by hampering the inflammatory cells. Moreover, the burnt skin tissue regenerated in vivo by the emulgel scaffold had similar structure and function to the neighboring tissue. This approach may contribute to the better understanding of the oil-loaded emulgel scaffold in skin tissue regeneration in the future.

Acknowledgments

Authors are grateful to the Vels Institute of Science, Technology & Advanced Studies (VISTAS), Chennai, for the facilities extended.

Declaration of Conflicting Interests

The author(s) declared no potential conflicts of interest with respect to the research, authorship, and/or publication of this article.

Funding

The author(s) received no financial support for the research, authorship, and/or publication of this article.

ORCID iD

T. S. Shanmugarajan https://orcid.org/0000-0003-0167-4579

References

1. Watts AM, Tyler MP, Perry ME, Roberts AH, McGrouther DA. Burn depth and its histological measurement. *Burns*. 2001;27:154-160.
2. Evans ND, Oreffo RO, Healy E, Thurner PJ, Man YH. Epithelial mechanobiology, skin wound healing, and the stem cell niche. *J Mech Behav Biomed Mater*. 2013;28:397-409.
3. Wang Y, Wang X, Shi J, et al. A biomimetic silk fibroin/sodium alginate composite scaffold for soft tissue engineering. *Sci Rep*. 2016;6:39477.
4. Diogo GS, Senra EL, Pirraco RP, et al. Marine collagen/apatite composite scaffolds envisaging hard tissue applications. *Mar Drugs*. 2018;16:E269.
5. Lu G, Ding Z, Wei Y, Lu X, Lu Q, Kaplan DL. Anisotropic biomimetic silk scaffolds for improved cell migration and healing of skin wounds. *ACS Appl Mater Interfaces*. 2018;10:44314-44323.
6. Lu D, Wang H, Wang X, et al. Biomimetic chitosan-graft-polypeptides for improved adhesion in tissue and metal. *Carbohydr Polym*. 2019;215:20-28.
7. Ojeh NO, Frame JD, Navsaria HA. In vitro characterization of an artificial dermal scaffold. *Tissue Eng*. 2001;7:457-472.
8. Heimbach DM, Warden GD, Luterman A, et al. Multicenter postapproval clinical trial of Integra dermal regeneration template for burn treatment. *J Burn Care Rehabil*. 2003;24:42-48.
9. Branski LK, Herndon DN, Pereira C, et al. Longitudinal assessment of Integra in primary burn management: a randomized pediatric clinical trial. *Crit Care Med*. 2007;35:2615-2623.
10. Xiong S, Zhang X, Lu P, et al. A gelatin-sulfonated silk composte based scaffold based on the 3D printing technology enhances the skin regeneration by stimulating epidermal growth and dermal neovascularization. *Sci Rep*. 2017;7:4288.
11. Jiang S, Lyu C, Zhao P, et al. Cryoprotectant enables structural control of porous scaffolds for exploration of cellular-mechano-responsiveness in 3D. *Nat Commun*. 2019;10:3491.
12. Mulye SP, Wadkar KA, Kondawar MS. Formulation, development and evaluation of indomethacin emulgel. *Der Pharmacia Sinica*. 2013;4:31-45.
13. Scholten HJ, Pierik RLM. Agar as a gelling agent: chemical and physical analysis. *Plant Cell Rep*. 1998;17:230-235.
14. Martín-López E, Darder M, Ruiz-Hitzky E, Sampedro MN. Agar-based bridges as biocompatible candidates to provide guide cues in spinal cord injury repair. *Biomed Mater Eng*. 2013;23:405-421.
15. Uppuluri VNVA, Shanmugarajan TS. Icariin-loaded polyvinyl alcohol/agar hydrogel: development, characterization, and in vivo evaluation in a full-thickness burn model. *Int J Low Extrem Wounds*. 2019;18:323-335.
16. Ishii F, Sasaki I, Ogata H. Effect of phospholipid emulsifiers on physicochemical properties of intravenous fat emulsions and/or drug carrier emulsions. *J Pharm Pharmacol*. 1990;42:513-515.
17. Maier C, Zeeb B, Weiss J. Investigations into aggregate formation with oppositely charged oil-in-water emulsions at different pH values. *Colloids Surf B Biointerfaces*. 2014;117:368-375.
18. Chung C, Koo CKW, Sher A, Fu JR, Rousset P, McClements DJ. Modulation of caseinate-stabilized model oil-in-water emulsions with soy lecithin. *Food Res Int*. 2019;122:361-370.
19. Gabás-Rivera C, Barranquero C, Martínez-Beamonte R, Navarro MA, Surra JC, Osada J. Dietary squalene increases high density lipoprotein-cholesterol and paraoxonase 1 and decreases oxidative stress in mice. *PLoS One*. 2014;9:e104224.
20. Katsarou AI, Kaliora AC, Chiou A, et al. Amelioration of oxidative and inflammatory status in hearts of cholesterol-fed rats supplemented with oils or oil-products with extra virgin olive oil components. *Eur J Nutr*. 2016;55:1283-1296.
21. Pal K, Banthia AK, Majumdar DK. Preparation and characterization of polyvinyl alcohol-gelatin hydrogel membranes for biomedical applications. *AAPS PharmSciTech*. 2007;8:21.

22. Singh VK, Pal K, Pradhan DK, Pramanik K. Castor oil and sorbitan monopalmitate based organogel as a probable matrix for controlled drug delivery. *J Appl Polym Sci*. 2013;130: 1503-1515.
23. Lou-Bonafonte JM, Martínez-Beamonte R, Sanclemente T, et al. Current insights into the biological action of squalene. *Mol Nutr Food Res*. 2018;8:e1800136.
24. Sagiri SS, Singh VK, Kulanthaivel S, et al. Stearate organogel-gelatin hydrogel based bigels: physicochemical, thermal, mechanical characterizations and in vitro drug delivery applications. *J Mech Behav Biomed Mater*. 2015;43: 1-17.
25. Shen CY, Dai L, Shen BD, et al. Nanostructured lipid carrier based topical gel of *Ganoderma* triterpenoids for frostbite treatment. *Chin J Nat Med*. 2015;13:454-460.
26. Bera H, Nadimpalli J, Kumar S, Vengala P. Kondogogu gum-Zn^{+2}-pectinate emulgel matrices reinforced with mesoporous silica for intragastric furbiprofen delivery. *Int J Biol Macromol*. 2017;104(pt A):1229-1237.
27. Yang H, Irudayaraj J, Paradkar MM. Discriminant analysis of edible oils and fats by FTIR. FT-NIR and FT-Raman spectroscopy. *Food Chem*. 2005;93:25-32.
28. Pourjavadi A, Farhadpour B, Seidi F. Synthesis and investigation of swelling behavior of new agar based superabsorbent hydrogel as a candidate for agrochemical delivery. *J Polym Res*. 2009;16:655-665.
29. Pradhan S, Sagiri SS, Singh VK, Pal K, Ray SS, Pradhan DK. Palm oil-based organogels and microemulsions for delivery of antimicrobial drugs. *J Appl Polym Sci*. 2014;131:39979.
30. Behera B, Biswal D, Uvanesh K, et al. Modulating the properties of sunflower oil based novel emulgels using castor oil fatty acid ester: prospects for topical antimicrobial drug delivery. *Colloids Surf B Biointerfaces*. 2015;128:155-164.
31. Salem HF, Kharshoum RM, Abou-Taleb HA, Naguib DM. Nanosized nasal emulgel of resveratrol: preparation, optimization, *in vitro* evaluation and *in vivo* pharmacokinetic study. *Drug Dev Ind Pharm*. 2019;9:1624-1634.
32. Zhang P, Chen L, Zhang Q, Hong FF. Using in situ dynamic cultures to rapidly biofabricate fabric-reinforced composites of chitosan/bacterial nanocellulose for antibacterial wound dressings. *Front Microbiol*. 2016;4:260.
33. Maharana V, Gaur D, Nayak SK, et al. Reinforcing the inner phase of the filled hydrogels with CNTs alters drug release properties and human keratinocyte morphology: a study on the gelatin-tamarind gum filled hydrogels. *J Mech Behav Biomed Mater*. 2017;75:538-548.
34. Khamrai M, Banerjee SL, Paul S, Samanta S, Kundu PP. Curcumin entrapped gelatin/ionically modified bacterial cellulose based self-healable hydrogel film: an eco-friendly sustainable synthesis method of wound healing patch. *Int J Biol Macromol*. 2019;122:940-953.
35. Ali NH, Amin MCIM, Ng SF. Sodium carboxymethyl cellulose hydrogels containing reduced graphene oxide (rGO) as a functional antibiofilm wound dressing. *J Biomater Sci Polym Ed*. 2019;30:629-645.
36. Gönüllü Ü, Üner M, Yener G, Karaman EF, Aydoğmuş Z. Formulation and characterization of solid lipid nanoparticles, nanostructured lipid carriers and nanoemulsion of lornoxicam for transdermal delivery. *Acta Pharm*. 2015;65:1-13.
37. Hussain A, Samad A, Singh SK, et al. Nanoemulsion gel-based topical delivery of an antifungal drug: in vitro activity and in vivo evaluation. *Drug Deliv*. 2016;23:642-647.
38. El-Refaie WM, Elnaggar YS, El-Massik MA, Abdallah OY. Novel curcumin-loaded gel-core hyaluosomes with promising burn-wound healing potential: development, in-vitro appraisal and in-vivo studies. *Int J Pharm*. 2015;486:88-98.
39. Tian M, Qing C, Niu Y, et al. The relationship between inflammation and impaired wound healing in a diabetic rat burn model. *J Burn Care Res*. 2016;37:e115-e124.
40. Abreu AM, Douglas de Oliveira DW, Marinho SA, Lima NL, de Miranda JL, Verli FD. Effect of topical application of different substances on fibroplasia in cutaneous surgical wounds. *ISRN Dermatol*. 2012;2012:282973.
41. Quinn KP, Golberg A, Broelsch GF, et al. An automated image processing method to quantify collagen fibre organization within cutaneous scar tissue. *Exp Dermatol*. 2015;24:78-80.
42. Oryan A, Mohammadalipour A, Moshiri A, Tabandeh MR. Topical application of *Aloe vera* accelerated wound healing, modeling, and remodeling: an experimental study. *Ann Plast Surg*. 2016;77:37-46.
43. Alam P, Ansari MJ, Anwer MK, Raish M, Kamal YK, Shakeel F. Wound healing effects of nanoemulsion containing clove essential oil. *Artif Cells Nanomed Biotechnol*. 2017;45:591-597.
44. Zhu X, Hu C, Zhang Y, Li L, Wang Z. Expression of cyclin-dependent kinase inhibitors, p21cip1 and p27kip1, during wound healing in rats. *Wound Repair Regen*. 2001;9:205-212.
45. Yang C, Zhu P, Yan L, Chen L, Meng R, Lao G. Dynamic changes in matrix metalloproteinase 9 and tissue inhibitor of metalloproteinase 1 levels during wound healing in diabetic rats. *J Am Podiatr Med Assoc*. 2009;99:489-496.
46. Martin LF, Rocha EM, Garcia SB, Paula JS. Topical Brazilian propolis improves corneal wound healing and inflammation in rats following alkali burns. *BMC Complement Altern Med*. 2013;13:337.
47. dos Santos JS, Monte-Alto-Costa A. Caffeic acid phenethyl ester improves burn healing in rats through anti-inflammatory and antioxidant effects. *J Burn Care Res*. 2013;34:682-688.
48. Zheng L, Hui Q, Tang L, et al. TAT-mediated acidic fibroblast growth factor delivery to the dermis improves wound healing of deep skin tissue in rat. *PLoS One*. 2015;10:e0135291.
49. de Loura Santana C, de Fátima Teixeira Silva D, de Souza AP, et al. Effect of laser therapy on immune cells infiltrate after excisional wounds in diabetic rats. *Lasers Surg Med*. 2016;48:45-51.
50. Shen HM, Chen C, Jiang JY, et al. The N-butyl alcohol extract from *Hibiscus rosa-sinensis* L. flowers enhances healing potential on rat excisional wounds. *J Ethnopharmacol*. 2017;198:291-301.
51. Chia CY, Medeiros AD, Corraes AMS, et al. Healing effect of andiroba-based emulsion in cutaneous wound healing via modulation of inflammation and transforming growth factor beta 31. *Acta Cir Bras*. 2018;33:1000-1015.
52. Alemzadeh E, Oryan A. Effectiveness of a *Crocus sativus* extract on burn wounds in rats. *Planta Med*. 2018;84:1191-1200.
53. Oryan A, Jalili M, Kamali A, Nikahval B. The concurrent use of probiotic microorganism and collagen hydrogel/scaffold enhances burn wound healing: an in vivo evaluation. *Burns*. 2018;44:1775-1786.